International Journal of Science and Research (IJSR)
ISSN: 2319-7064
ResearchGate Impact Factor (2018): 0.28 | SJIF (2019): 7.583

Geometric Correction Algorithm for Hyperspectral Images based on GPS

WANG Li[1], WANG Wei[2], LIU Boni[3]

[1] Xi'an Aeronautical University, Department of Electronic Engineering, Xi'an Shaanxi 710077, China

Abstract: ***A geometric correction algorithm based on GPS for the hyperspectral images acquired by push-broom imaging spectrometer is proposed. The correction method consists of three steps, namely, data import, coordinate computing and image correction. Data import read hyperspectral data and attitude information data given by GPS; coordinate computing calculates the Gaussian plane rectangular coordinates for each pixel in the image; while image correction calculates the corresponding coordinate in the corrected image of the pixels according to the Gaussian plane rectangular coordinates and using the nearest neighbor interpolation method to smooth the image. The corrected results show that the algorithm is ideal for hyperspectral image geometric correction, and the algorithm is computational efficiency.***

Keywords: Hyperspectral Image; GPS; Data Import; Coordinate computing; Imaging Correction

1. Introduction

The imaging spectrometer combines imaging technology and spectroscopic technology, making remote sensing technology enter a new stage that can simultaneously obtain spectral information and spatial distribution characteristic information of the earth's surface matter. The sensors of the imaging spectrometer detect the reflection or radiation intensity of the ground object or target to hundreds of different wavelengths, and form a spectral image composed of hundreds of continuous spectral bands. Hyperspectral remote sensing images are defined as three-dimensional stereo data composed of two-dimensional spatial domains and one-dimensional spectral domains. Unlike video sequence images, the images in the spectral domains of the hyperspectral remote sensing images have the same position in the spatial domain, that is, high spectral remote sensing images are composed of images of different spectral bands in the same field of view 0[2].

The main imaging methods of hyperspectral imagers are push-broom linear array scanning and push-broom area array scanning. The push-broom spectrometer generates hundreds of continuous spectral bands. After being separated by the optical dispersive device, radiation in different bands is irradiated onto the elements of the line array, and the entire image is acquired by progressive scanning. The push-broom area scan method records the data line by line, no longer moving components, and directly acquiring images. Due to the high spectral resolution of the hyperspectral image, it has great potential for civilian and military use, but due to factors such as the imaging device's shooting attitude and scanning non-linearity, the resulting hyperspectral remote sensing image will have geometric distortion and cannot meet the application in specific fields. Therefore, geometric correction is one of the problems that must be solved to realize the application of hyperspectral remote sensing technology. Compared with satellite remote sensing sensors, the airborne imaging spectrometer has the characteristics of poor imaging platform stability and low flying height. The combination of these factors complicates the geometric distortion of the acquired hyperspectral remote sensing image. The purpose of geometric correction is to eliminate these geometries distortion as much as possible.

In the absence of accurate position parameters, only tangent correction and yaw correction can be used to make preliminary corrections to remote sensing images. The geometric correction algorithm of remote sensing image based on support vector machine was studied in [3]. The coordinates of ground control points were measured using differential GPS, and then the image was geometrically corrected using remote sensing image processing software. Cao [4] also carried out research on the geometric correction of remote sensing images, and realized rapid processing of remote sensing images. In terms of hyperspectral image correction, Yi [5] combined the control points and digital elevation models to complete the geometric fine correction of CASI hyperspectral images. Literature [6] proposed direct method and indirect method for the correction of hyperspectral images without stable platform. A hyperspectral imaging system that uses an indoor imaging spectrometer to collect data on a multi-rotor UAV is proposed in [7]. In the algorithm, control points and standard gray cloth are placed in the test area, and GPS-RTK is used to measure the three-dimensional coordinates of the control points, the reflectance of standard gray cloth is measured to verify the imaging accuracy of the system. However, the correction accuracy of these correction methods is greatly affected by the selection of control points, the accuracy is not high, and manual calibration and field measurement of a large amount of ground control information are required, which is time-consuming. A correction algorithm on processing drone-borne hyperspectral data [7] is proposed by Jakob, and an approach to atmospheric correction for hyperspectral imagery in the long wave infrared spectral band requiring the estimation of the atmospheric optical parameters (AOP) is proposed in [9]. Li established a UAV remote sensing image based on flight attitude changes combined with a correction model [10], which improved the speed and accuracy of preprocessing of UAV remote sensing data in the absence of ground control points. However, the algorithm accuracy has a lot to do with changes in flight parameters.

Aiming at the hyperspectral remote sensing images obtained by the push-broom imaging spectrometer, a geometric correction algorithm based on synchronized high-precision GPS (recording the attitude information data of the imaging platform) is proposed. Without manual intervention, the algorithm could correct the hyperspectral images at high precision, which overcomes the shortcomings of the traditional polynomial correction method, such as the difficulty in obtaining the ground control point information and the low accuracy of the correction.

2. The proposed correction algorithm

2.1 System composition

The schematic diagram of the hyperspectral remote sensing imaging system is shown in Figure 1. The imaging spectrometer and high-precision GPS are mounted on the bottom of the aircraft. The Resonon pika series hyperspectral imager made in the United States was selected in the experiment [11]. The imaging spectrometer obtains hyperspectral remote sensing images by push-broom method, and finally obtains standard data files and corresponding data header files of hyperspectral remote sensing images stored in bil format. The high-precision GPS records the attitude of the imaging platform when the imaging spectrometer is pushed in the imaging process.

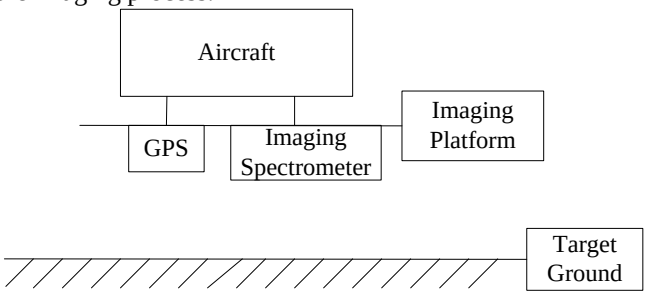

Figure 1: Hyperspectral imaging system.

In the process of pushing and sweeping, the influence of the remote sensing platform on the geometric deformation of the image mainly includes:

(1) Pitch angle: the angle between the aircraft's longitudinal axis and the horizontal plane. The change of aircraft pitch angle is one of the main sources of geometric distortion of hyperspectral scanned images, which will cause geometric distortion of images in the scanning direction and heading. In the scanning direction, the change of the pitch angle changes the actual observation distance to the ground, resulting in a corresponding increase or decrease of the ground scanning width. In the course, the change of the pitch angle results in the shift of the scanning line position, causing the scanning line to be shifted overlap or gap.

(2) Roll angle: the angle between the horizontal axis of the aircraft and the horizontal plane. The change of the roll angle causes the position of the scan starting point to be shifted, resulting in distortion of the features on the image. The change of roll angle does not affect the image in the heading direction, but causes considerable image distortion in the scanning direction.

(3) Yaw angle: the angle between the direction of aircraft movement and the true north position. The yaw angle makes the real track of the aircraft deviate from the original course, which causes severe geometric distortion of the remote sensing image.

In view of the above analysis, the main function of the GPS system is to record the attitude information of the remote sensing platform, including: pitch angle ψ, roll angle ω, yaw angle κ, and the unit is rad. At the same time, the corresponding latitude, longitude and altitude H must be recorded.

2.2 Geometric correction algorithm

In order to obtain a hyperspectral image that accurately reflects the surface conditions, the necessary geometric corrections must be performed. In order to ensure the accuracy and quality of geometric correction, it is usually necessary to perform geometric fine correction processing on hyperspectral images. This paper uses the platform attitude information recorded by GPS to correct the original image into the required map projection coordinate system. This process mainly includes three steps, which are data import, coordinate computing and image correction. The diagram of the correction algorithm is shown in Figure 2. The details are summarized as follows.

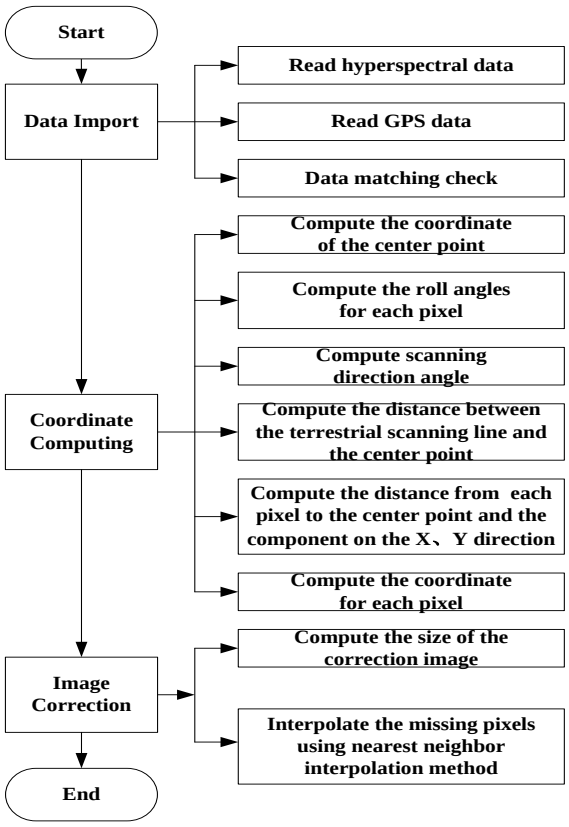

Figure 2: The diagram of the correction algorithm.

2.2.1 Data import

The storage of hyperspectral data includes three formats, namely bil, bsq, and bip. The hyperspectral image data obtained by the imaging spectrometer in the system in this paper is the bil format [12]. The hyperspectral data was read using matlab to obtain three-dimensional data cubes. At the same time, the attitude information data of the remote sensing

platform recorded by GPS were read. It should be noted that, because the number of attitude information data recorded by GPS and the number of scan lines when the imaging spectrometer acquires hyperspectral remote sensing images may be inconsistent, it is necessary to resample the attitude information data recorded by GPS to make the two matching.

2.2.2 Coordinate computing

The observed value of the GPS satellite positioning system is the measured value in the WGS-84 geodetic coordinate system. In the image processing analysis, the coordinate system used is a Gaussian plane rectangular coordinate system. Therefore, before geometric correction of the image, with the help of latitude and longitude provided by GPS, and the pitch angle, roll angle and yaw angle of the remote sensing platform, the Gaussian plane rectangular coordinates corresponding to each image pixel point must be calculated.

According to the longitude and latitude of the center point of the scanning line m (initial value $m=1$), its corresponding Gaussian plane rectangular coordinates is calculated as:

$$X = \alpha + L^2 \times \beta \times \sin B \times \cos B/2 + L^4 \times \beta \times \sin B \cos^3 B \times \left(5 - \tan^2 B + 9\eta^2 + 4\eta^4\right)/24 + L^6 \times \beta \times \sin B \cos^5 B \times \left(61 - 58\tan^2 B + \tan^4 B\right)/720 \quad (1)$$

$$Y = L \times \beta \times \cos B + L^3 \times \beta \times \cos^3 B\left(1 - \tan^2 B + \eta^2\right)/6 + L^5 \times \beta \times \cos^5 B \times \left(9 - 18\tan^2 B + \tan^4 B\right)/120 + 500000 \quad (2)$$

$$L = L_1 - L_c \quad (3)$$

$$\alpha = a_1 \times B + b_1 \times \sin(2B) + c_1 \times \sin(4B) + d_1 \times \sin(6B) \quad (4)$$

$$\beta = 6399698.902 - 21562.267 \times \cos^2 B + 108.973\cos^4 B - 0.612\cos^6 B \quad (5)$$

$$\eta = 0.0067385254 \times \cos^2 B \quad (6)$$

Where, X is the Vertical (North-South) direction, Y is the horizontal (east-west) direction; B is the latitude (rad) of the center point of the scanning line m; L_1 is the longitude (rad) of the center point of the scanning line m; L_c is the center longitude of the projection band formed by all scanning lines; $a_1 = 6367558.5, b_1 = -16036.48, c_1 = 16.828, d_1 = -0.022$

According to the Gaussian plane rectangular coordinates of the center point of the scan line, combined with the attitude information obtained by GPS measurement, the Gaussian plane rectangular coordinates corresponding to all the pixels on the scanning line m could be calculated. The steps are as follows.

Step 1: Calculate the direction angle of the scanning line m,

$$\gamma = \kappa + \pi/2 \quad (7)$$

Where, κ is the yaw angle of scan scanning m.

Step 2: Calculate the distance from the center point of the scanning line m to the center point of the corresponding ground scanning line:

$$D = H/\cos\psi \quad (8)$$

Where, H and ψ are the altitude and pitch angle of the scanning line m.

Step 3: Calculate the roll angle of the i th pixel of the scanning line m:

$$\omega_i = \omega - (N-1) \times IFOV/2 + i \times IFOV \quad (9)$$

Where, i is the pixel number from the left of the scanning line, initial value is $i=1$; N is the detection elements of imaging spectrometer line array; ω is the yaw angle corresponding to the center point of the scanning line m; $IFOV$ is instantaneous field of view of imaging spectrometer.

Step 4: Calculate the distance S_i between the i th pixel and the center point of the scanning line m. In addition, its Gaussian plane rectangular coordinate components in north-south and east-west directions, denoted as Δx_i and Δy_i, are computed.

$$S_i = D \times \tan(\omega_i) \quad (10)$$

$$\Delta x_i = S_i \times \cos(\gamma) \quad (11)$$

$$\Delta y_i = S_i \times \sin(\gamma) \quad (12)$$

Step 5: Calculate the Gaussian plane rectangular coordinates corresponding to the i th pixel of the scanning line m,

$$x_i = X + \Delta x_i \quad (13)$$

$$y_i = Y + \Delta y_i \quad (14)$$

Repeat the above steps, make $i = i+1$, calculate the rectangular coordinates of the Gaussian plane corresponding to all the pixels of the scanning line m. Apply this method, we can calculate the Gaussian plane rectangular coordinates corresponding to all the pixels in all scanning lines of the hyperspectral remote sensing image.

2.2.3 Image correction

According to the Gaussian plane rectangular coordinates of each pixel, the position and gray level of each pixel in the corrected image are calculated. First determine the size of the corrected image according to the maximum and minimum Gaussian plane rectangular coordinates corresponding to all pixels:

$$xsize = (x\max - x\min)/GR \quad (15)$$

$$ysize = (y\max - y\min)/GR \quad (16)$$

$$GR = 2 * \overline{H} * \tan(IFOV/2) \quad (17)$$

Where, $y\max$ and $y\min$ represent the maximum and minimum coordinates of all pixels in the horizontal direction. $x\max$ and $x\min$ represent the maximum and minimum coordinates of the north and south directions, respectively. GR is the pixel resolution corresponding to the spectrometer, and $\overline{H}$ is the average altitude corresponding to all scan lines.

The calculated $xsize$ and $ysize$ is the number of rows and columns of the corrected image. According to (15) and (16),

we can compute the rows and columns corresponding to each pixel in the corrected image. The pixel values of the hyperspectral remote sensing image obtained by the imaging spectrometer are assigned to the corresponding pixels in the corrected image. Due to the inconsistent image size before and after correction, there are missing pixels in the corrected image data, and the nearest neighbor interpolation method [13] is used to eliminate it.

3. Experimental Results and Analysis

The first experimental data of remote sensing platform is vehicle-mounted, that is, the spectral imager is mounted on the top of the car, and the movement of the car is used to complete the sweep of the spectrometer, and then acquire the image. Before the experiment, the target shown in Figure 3 (a) was laid on the ground, and the center line of the target was parallel to the solid white line on the roadside. To simulate the unstable movement of the imaging platform, the car's trajectory during the imaging process is S-shaped. The obtained hyperspectral remote sensing image is shown in Figure 3 (b). The target in the image is severely deviated from its true position. The proposed algorithm is used for geometric correction and the correction result is shown in Figure 3 (c). Seen from the correction image, the centerline of the target and the solid white line on the side of the road are parallel to each other, which is in good agreement with the actual ground experiment laying situation. The results fully illustrate the effectiveness of the correction algorithm. The remote sensing platform for the second experimental data is airborne, that is, the spectral imager is mounted on an aircraft, and the aircraft moves to complete the sweep of the spectrometer. We take the area shown in Figure 4 (a) as the target image, and the obvious landmark in the imaging area is the two oval playgrounds. The hyperspectral remote sensing image obtained by aerial photography is shown in Fig. 4 (b). During the imaging process, the hyperspectral image acquired has different degrees of deformation due to the unstable imaging platform. Compared with figure (a), the shape of the playground on the lower side of the image is much different from the actual playground. The proposed algorithm is used to geometrically correct the hyperspectral remote sensing image. The correction results obtained are shown in Figure 4 (c). Compared with the target image, the correction result is very ideal, which is in good agreement with the real map.

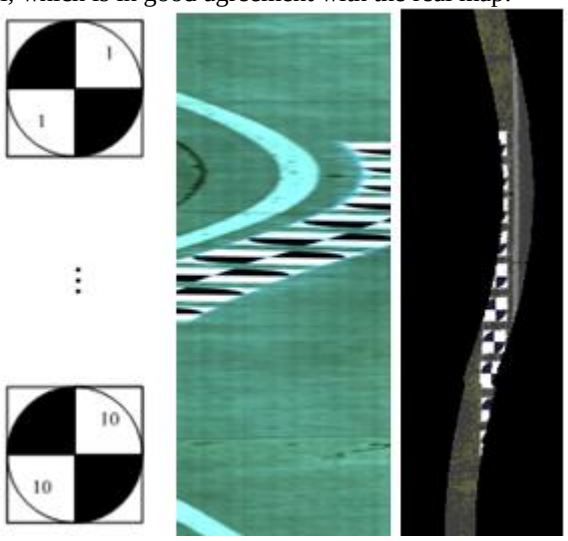

(a) target image (b) real hyperspectral image (c) correction image

Figure 3: The comparison of the original image and the correction image.

The correction results in this paper are calculated using matlab. The computer memory is 16G, the processor is AMD Athlon (tm) II, and the main frequency is 3GHz. The time for calculating the second set of experimental data is about 2 minutes for each band. The calculation efficiency is high, which can meet the needs of real-time image processing. At the same time, the correction method does not require manual intervention. After the original image data and the matching GPS attitude information data are given, the computer can complete the image correction.

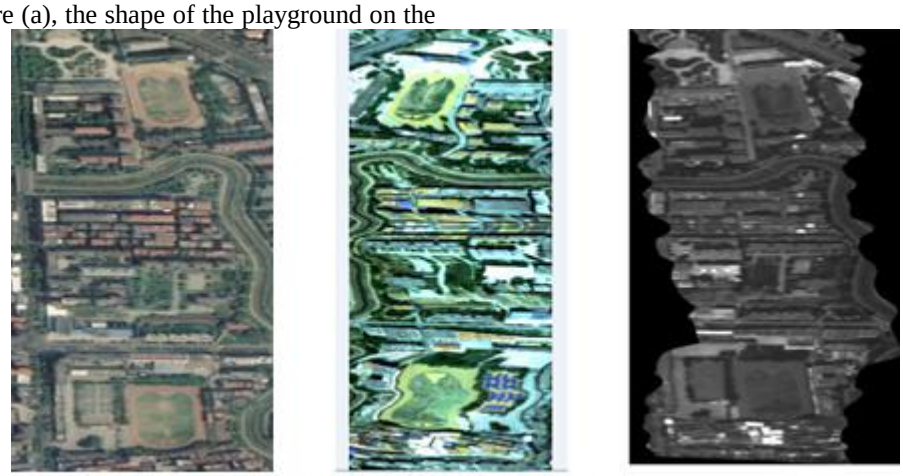

(a) target image (b) real hyperspectral image (c) correction image

Figure 4: The comparison of target image and correction image.

4. Conclusions

The geometric correction of hyperspectral images is the basis for carrying out research on the application of hyperspectral data, to achieve an effective combination of hyperspectral data and its spatial positioning, preparing for the continious spectral analysis and matching. The geometric correction algorithm for hyperspectral remote sensing images proposed

in this paper, utilizes the high-precision GPS recorded position information data of the imaging platform to geometrically correct the distortion caused by the unstable movement of the platform. The computation complexity is low due to the small amount imaging platform's pose information data; therefore it can meet the needs of real-time correction of the image. The correction results show that the method can correct the geometric distortion caused by the unstable movement of the imaging platform, and does not depend on the selection of ground control points. The correction results are in good agreement with the real map, and the correction accuracy is high.

5. Acknowledgements

This work was supported by the National Natural Science Foundation of China (grant number 61901350); Scientific Research Plan Projects of Shaanxi Education Department (grant number 19JK0432) and Science Research Fund of Xi'an Aeronautics University (grant number 2019KY0208).

References

[1] Ren Z, Wu L. Spectral-spatial Classification for Hyperspectral Imagery Based on Intrinsic Image Decomposition [J]. Spacecraft Recovery & Remote Sensing, 2019, 40(3): 111-120. DOI:10.3969/j.issn.1009-8518.2019.03.014.
[2] Chang C I. A Review of Virtual Dimensionality for Hyperspectral Imagery [J]. IEEE Journal of Selected Topics in Applied Earth Observations and Remote Sensing, 2018, 11(4): 1285-1305.
[3] Sun J. Research about the algorithms of the remote image geometry correction based on support vector machines [D]. Xi'an: Xi'an University of Science and Technology, 2011: 8-16.
[4] Cao Ling-ling, Study and implementation on rapidly processing method of remote image [D]. Taiyuan: North University of China, 2011:7-27.
[5] Yi Pi-yuan, Tong Peng, Zhao Ying-jun, Li Han-bo, Wu Wen-huan. LiDAR Assisted Geometric Accurate Correction of Airborne Hyperspectral Image [J]. Science Technology and Engineering, 2019, 19(14): 22-28. DOI:10.3969/j.issn. 1671-1815.2019.14.004.
[6] Zhang Hao, Zhang Bing, Wei Zheng. Fast rectifying hyperspectral image based on POS system [J]. Bulletin of surveying and mapping, 2009, (1): 14-17.
[7] Zhou Rui, Ou Yi, Yu Bao. Research of Geomatric and Radiation Correction of the Hyperspectral Imaging System Carried by a Multi-rotor Unmanned Aerial Vehicle [J]. Journal of Southwest University (Natural Science), 2019, 41(9):141-147. DOI:10.13718/j.cnki.xdzk. 2019.09.018.
[8] S. Jakob, R. Zimmermann and R. Gloaguen. Processing of drone-borne hyperspectral data for geological applications [C]. 2016 8th Workshop on Hyperspectral Image and Signal Processing: Evolution in Remote Sensing (WHISPERS), Los Angeles, CA, 2016, pp. 1-5.
[9] P. Lahaie. Autonomous Atmospheric Correction Algorithm for Long Wave Infrard Hyperspectral Imagery [C]. 2018 9th Workshop on Hyperspectral Image and Signal Processing: Evolution in Remote Sensing (WHISPERS), Amsterdam, Netherlands, 2018, pp. 1-5.
[10] Li Zheng. Geometric correction algorithm for unmanned aerial vehicle remote sensing image without ground control points [D]. Chengdu: University of electronic science and technology of china, 2010: 30-36.
[11] http://www.instrument.com.cn/netshow/SH101449/C138506.htm.
[12] Resonon. Airborne Spectral Imaging System User Manual [M]. 2011.
[13] Feng Bo, Chen Mingtao, Yue Dongdong, Li Shengtao, Jia Xiaofeng, Song Dan. Comparison of 3D Geological Modeling Based on Two Different Interpolation Methods [J]. Journal of Jilin University (Earth Science Edition), 2019, 49(4): 1200-1208. DOI:10.13278/j.cnki.jjuese.20180250.

Author Profile

WANG Li received the B.E. degree in electronic and information engineering from Xi'an University of Architecture and Technology, Xi'an, China, in 2009 and the M.S. degree in signal and information processing from Beihang University, Beijing, China, in 2012. She received the Ph.D. degree from Northwestern Polytechnical University, Xi'an, China, in 2018. She now is a lecturer in Xi'an Aeronautics University. Her research interests include compressed sampling, hyperspectral image processing, and optimization algorithm.

WANG Wei received the B.E. degree in electronics and information technology, the Master's degree in aerospace propulsion theory and engineering and the Ph.D. degree in electronic science and technology from the Northwestern Polytechnical University, Xi'an, China. Since 2015, he has been a lecturer in Xi'an Aeronautics University. His current research interests include antenna and radome design, electromagnetic scattering analysis and intelligent optimization algorithm.

LIU Boni received the B.E. degree in Technique of Measuring Control and Instrument from Xi'an Shiyou University, Xi'an, China, in 2003 and the M.S. degree in geodesy and engineering major from Xi'an University of Science and Technology, Xi'an, China, in 2006. Since 2006, she has been a lecturer in Xi'an Aeronautics University. Her research interests include communication technology and electronic measurement.